Production of Hydrophobic Surfaces in Biodegradable and Biocompatible Polymers Using Polymer Solution Electrospinning

L. Buruaga, A. González, L. Irusta, J. J. Iruin

Department of Polymer Science and Technology and Institute for Polymer Materials (POLYMAT), University of the Basque Country, 20080 San Sebastián, Spain

ABSTRACT: In this work, the electrospinning of polymer solutions was used to produce mats with hydrophobic properties from a series of commercially available biodegradable and biocompatible polymers, such as poly(3-hydroxybutyric acid-*co*-3-hydroxyvaleric acid), poly (DL-lactide), polycaprolactone, and poly(L-lactide). According to the results, to obtain hydrophobic properties, bead-like morphologies were the most adequate. For obtaining this type of morphology, the polymer concentration of the electrospun solution had to be sufficiently low, although below a limit concentration it was not possible to obtain hydrophobic surfaces. The results also showed that the crystallinity of the materials may influence the final hydrophobic properties. © 2010 Wiley Periodicals, Inc. J Appl Polym Sci 120: 1520–1524, 2011

Key words: electrospinning; hydrophobic; biodegradable

INTRODUCTION

Surfaces with very high water static contact angles (CAs) (larger than 150°) and hysteresis values (difference between the advancing and receding angles) lower than 10° are usually called superhydrophobic surfaces. These surfaces are of special interest because properties such as antisticking, anticontamination, and self-cleaning are expected.[1–3] In the nature, many plant surfaces exhibit water repellent properties, but the lotus leaves are the most famous example. The hydrophobic nature of the lotus leaf can be attributed not only to a low surface energy but also to a surface roughness on at least two different length scales (micrometer and nanometer).[4] Mimicking nature, many researchers have studied different methods for producing superhydrophobic surfaces. In practice, superhydrophobic surfaces can be prepared using different methods such as etching[5] and lithography,[6] sol–gel processing,[7,8] and electrospinning.[9]

Electrospinning is a process that creates ultrafine fibers through an electrically charged jet of polymer solution.[10] Depending on the solution concentration, the obtained mats may exhibit fiber or fiber–bead morphologies.[11] According to several groups,[12,13] a dual structure made of fibers and beads should be used to provide sufficient surface roughnesses for superhydrophobicity. Rutledge and coworkers[14] described two different strategies to make hierarchically roughened superhydrophobic surfaces, particularly in the form of electrospun nonwoven mats, by decorating micrometer-scale fibers with nanometer-scale pores or particles. The effect of the secondary roughness in the hydrophobic behavior of the obtained mats is a question of growing interest, and, therefore, several works are being published.

In this work, the electrospinning technique was used to produce mats with hydrophobic properties from a series of commercially available biodegradable and biocompatible polymers. The effect of the polymer concentration and its chemical nature on the obtained morphology was related to the wettability of the mat. The selected polymers were all poly(esters) based on polylactide (PLA), polycaprolactone (PCL), and poly(hydroxyalkanoate)s that have been extensively used as biomaterials.

EXPERIMENTAL

Materials

Poly(3-hydroxybutyric acid-*co*-3-hydroxyvaleric acid), with PHV content 5 wt % (PHV5), poly(DL-lactide) (PDLA) with nominal weight-average molecular weight M_w 75,000–120,000, polycaprolactone with

TABLE I
Electrospinning Parameters and Minimum Concentration for Obtaining a Fiber-Like Morphology (C_i) of the Described Polymers

Polymer	C_i (wt %)	Flow rate (mL/h)	Voltage (kV)
PHV5	3	0.10	5
PCL	7	0.50	5
PLLA	2	0.50	3
PDLA	15	0.25	7

nominal number-average molecular weight M_n 70,000–90,000, and chloroform (HPLC grade) were purchased from Aldrich Chemical Corporation. Poly(L-lactide) (PLLA) with nominal weight-average molecular weight 300,000 was purchased from Polyscience. All materials were used as received. Water was doubly distilled and deionized (Millipore, Milli-Q).

Electrospinning

The polymers were dissolved at different concentrations in chloroform by gently stirring with a magnetic bar at room temperature and atmospheric pressure.

For the electrospinning process, polymer solutions were placed into a syringe with an 18-gauge blunt-end needle that was mounted in a syringe pump (Cole-Parmer). Nanofibers were electrospun by applying a voltage between 3 and 7 kV to the needle, using a Spellman CZE1000R high voltage supply (0–30 kV CZE1000R; Spellman High Voltage Electronics), with a low current output (limited to a few microamperes). The ground plate was placed at 13 cm from the needle tip and was kept constant in all the experiments. The syringe pump delivered the polymer solutions at a controlled flow rate, ranging from 0.10 to 0.50 mL/h. All the experiments were performed at least twice. The resulting fibers were collected on the screen to produce a sheet of nonwoven fabric.

Characterization techniques

Static and dynamic water CA measurements were carried out using the sessile drop method on a OCA20 contact angle goniometer at 25°C and 55% of relative humidity. The angles reported were the average of 30 measurements.

Fiber morphology was characterized by scanning electron microscopy (SEM). The measurements were performed in a Hitachi S-2700 microscope, by placing the samples on a SEM disk and sputter-coated with an 8-nm Pt/Au layer.

Differential scanning calorimetric (DSC) studies were carried out in a DSC Q 2000 from TA instruments at a heating rate of 10°C/min. Crystalline degree was estimated relating melting enthalpies

calculated in the first run with melting enthalpy of 100% crystalline polymer previously reported (136 J/g for PCL,[15] 146 J/g for PHV5,[15] and 93 J/g for PLLA[16]).

RESULTS AND DISCUSSION

Using the methodology described in previous works,[11,17] the minimum concentration for obtaining a fiber-like morphology (C_i) was determined for all the investigated polymers. Table I summarizes the obtained results.

To change the morphology of the mats, different solutions were prepared for each polymer, at concentrations lower and higher than C_i. The solutions were then electrospun using the parameters described in Table I, and the water CA was measured. Flat films were also prepared by a simple spreading of the solutions onto a glass surface and subsequent drying at room temperature for 48 h. The water CA of the flat surfaces was also determined. Table II shows the obtained results.

As can be observed in Table II, in spite of the high error bar involved in the measurements, the water CA increased when the polymer concentration was decreased. High CAs were obtained at low concentrations, especially with PHV5, PCL, and PLLA. Moreover, regardless of the polymer nature and concentration, the mats showed water CAs considerably higher than those obtained with films of the same polymer. The electrospun surfaces exhibited water CAs characteristic of hydrophobic surfaces; meanwhile, the flat surfaces gave rise to hydrophilic surfaces.

However, the superhydrophobicity is not only defined by high static CA values but also by hysteresis values (difference between the advancing and receding angles) lower than 10°. Low hysteresis values are governed by the Cassie state in which water droplets are in contact with peaks of the

TABLE II
Description of the Electrospun Samples and Water Contact Angles of the Mats and Flat Surfaces (Films)

Polymer	Concentration (wt %)	Contact angle of film (°)	Contact angle of mats (°)
PHV5	0.75	–	144 ± 10
	1.5	87 ± 10	139 ± 10
	3	–	129 ± 5
	4	–	121 ± 4
PCL	4	66 ± 10	159 ± 10
	6	–	132 ± 6
	8	–	127 ± 5
PLLA	1.5	70 ± 3	141 ± 6
	2	–	131 ± 5
PDLA	10	–	120 ± 5
	15	74 ± 8	111 ± 2
	20	–	105 ± 4
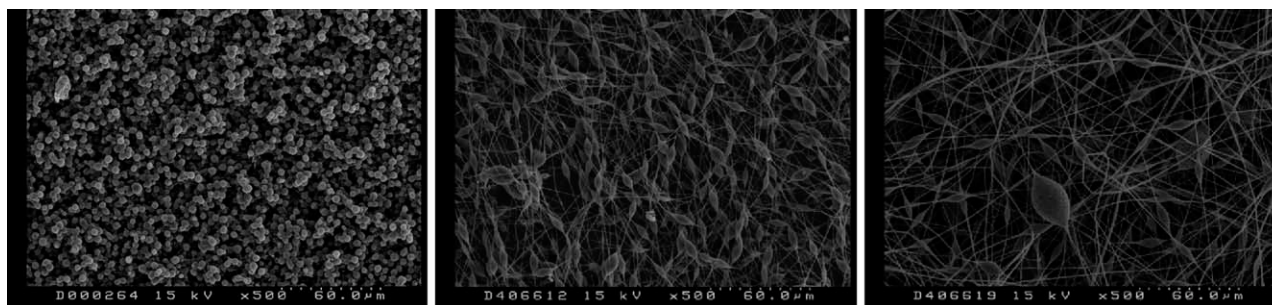
Figure 1 SEM images of the mats obtained from PHV5 using a concentration of 0.75 wt % (left), 3 wt % (center), and 4 wt % (right).

rugged surface as well as the "air pockets" trapped between surface grooves. In the Cassie state, the liquid droplet slides off easily even if the film is only slightly tilted. According to this, the hysteresis values of the mats that gave rise to higher static CAs were determined. For the mats obtained from PHV5 and PLLA at the lower concentration (0.75 and 1.5 wt %), the hysteresis values were 6.1° ± 1.0° and 7.7° ± 1.0°, respectively. However, for the mat obtained from PCL at 4 wt %, the hysteresis value was higher than 10 (11.4° ± 0.9°), and therefore although this mat showed the highest static CA (159°), the hysteresis value is slightly larger than the required to be considered as superhydrophobic.

The high CAs obtained in the electrospun surfaces could be related to the morphology of the surface. Figure 1 shows the SEM images of the mats obtained from PHV5 using different starting concentrations.

The image of the mat obtained from the lower concentration solution showed a bead-like morphology with an average bead diameter lower than 4 μm. When the concentration was increased, beaded fibers were observed with a fiber diameter lower than 2 μm. It is important to remind that the films obtained from 0.75, 3, and 4 wt % solutions had CAs of 144°, 129°, and 121°, respectively. The above results revealed that a bead-predominant morphology generates larger CAs than those generated on a morphology mainly consisting on fibers, as it was previously stated in literature.[12]
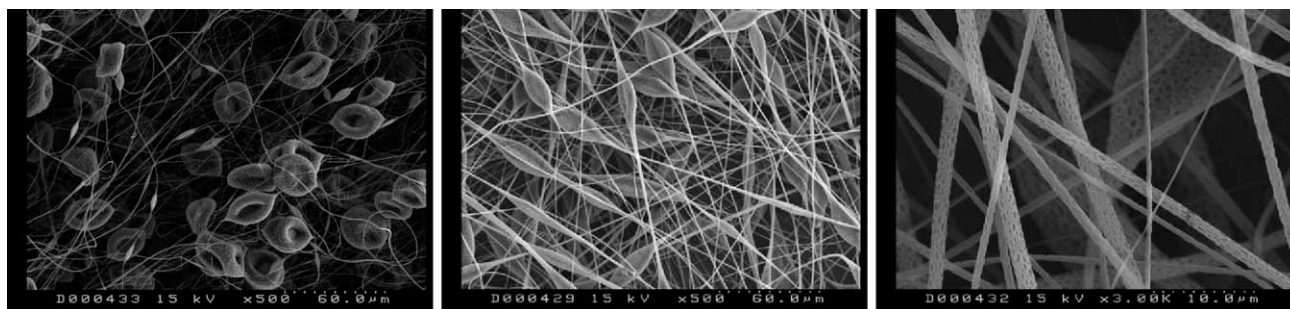
Figure 2 shows the images of the mats obtained from PCL solutions. As in the previous case, when the concentration was increased, the morphology of the mats changed from beads to fibers. Moreover, the larger CA (159°) was obtained at a low concentration (4%) where the bead-predominant morphology was observed. In this sample, spherical beads with an average bead diameter lower than 20 μm were observed. Over some of these beads, smaller beads were deposited (1–5 μm). Moreover, some nanometer-diameter fibers were around the small beads. It seems that this particular morphology was responsible for obtaining high CA.

The SEM images of the mats obtained using a PCL concentration of 8 wt % (Fig. 2, right) showed fibers with nanometer-scale pores. These types of structures have been previously described in literature[14,18] and have been related to the high volatility of the solvent and to the relative humidity of the air during the electrospinning process. The approach of introducing pore structures on electrospun fibers has the practical advantage of achieving hierarchically roughened fabrics in a single process step, but the enhancement in hydrophobicity resulting from the introduction of pores is modest. In our case, the CA of the pore-containing fibers was 127°, lower than those obtained when a bead-like morphology was presented (157°, 4 wt %). Once again, bead-predominant morphology generated larger CAs. Unfortunately, it was not possible to obtain fibers without
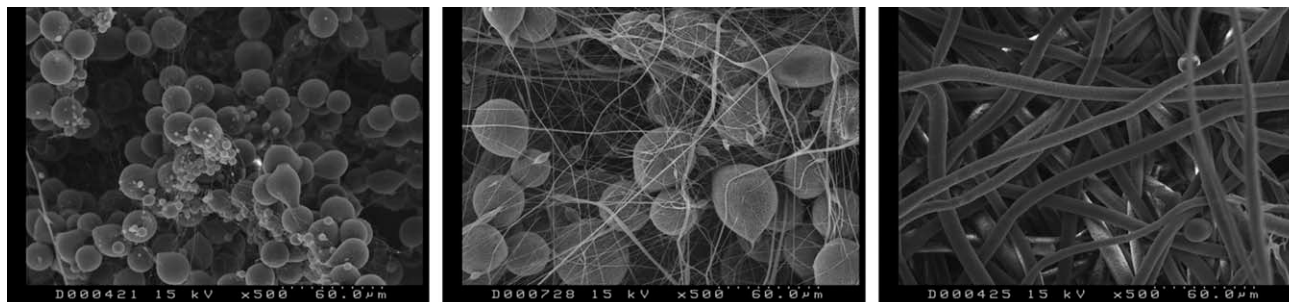
Figure 2 SEM images of the mats obtained from PCL using a concentration of 4 wt % (left), 6 wt % (center), and 8 wt % (right).

Figure 3 SEM images of the mats obtained from PLLA using a concentration of 1.5 wt % (left), 2 wt % (center), and 2 wt %, higher magnification (right).

pores and, therefore, the effect of the pores in the hydrophobicity could not be stated.

Figure 3 shows the SEM images of the mats obtained from PLLA solutions. As can be observed, using a concentration of 1.5 wt %, a morphology based on beads and fibers was obtained. The beads were oval shaped, showing a size lower than 30 μm with nanometer-scale pores. Increasing the concentration to 2 wt %, porous fibers were obtained. As in the previous systems, the CA of the mats with fiber-like morphologies was lower than that obtained in the mats with a beaded morphology. It is interesting to remark that the values of the CAs registered when a fiber-like morphology was obtained were very similar (≈130°), regardless of the chemical nature of the fiber.

Finally, Figure 4 shows the SEM images of the fibers obtained from PDLA solutions. As can be seen in Figure 4, as the polymer concentration increased, the morphology of the mats changed from beads to fibers. Moreover, and according to Table II, the CA of the mats increased when the polymer concentration decreased. However, the CAs obtained using PDLA solutions were, in all cases, lower than those obtained with the previously mentioned polymers. This result is not easy to explain. The CA of the flat film obtained from PDLA was very similar to those obtained using PLLA, and, therefore, the chemical nature of the polymer cannot be responsible for obtaining lower water CAs in the mats. In addition, the morphology of the

PDLA mats did not show significant changes comparing with that of the other polymers, and, therefore, the great decrease in the CA cannot be exclusively attributed to the surface morphology.

The PDLA is obtained from the racemic mixture of D and K lactides, and, therefore, the obtained polymer is amorphous; meanwhile, the PLLA obtained from L-lactide is a semicrystalline polymer. According to literature,[18] the microstructure and nanostructure of crystals can be responsible for hydrophobicity. Taking into account this fact, the lower CA obtained in the PDLA mats could be related with the amorphous nature of the polymer. It is important to point out that the PDLA is the only amorphous polymer used in our work. The melting point (T_m) and the crystallinity degree (%X) of the mats obtained from the lower polymer concentration of PHV5, PCL, and PLLA were measured by DSC. The obtained values were as follows: PHV5: $T_m = 159°C$, %$X = 60\%$; PCL: $T_m = 62°C$, %$X = 52\%$; and PLLA: $T_m = 176°C$, %$X = 23\%$. According to this, the high CA observed in the mats obtained from PHV5, PCL, and PLLA could be related to the polymer crystallinity. However, the high polymer concentration used for obtaining amorphous PDLA mats could also be responsible for the lower CA.

The results obtained showed that, to obtain hydrophobic properties, bead-like morphology was the most adequate and that for obtaining this morphology the polymer concentration of the electrospun
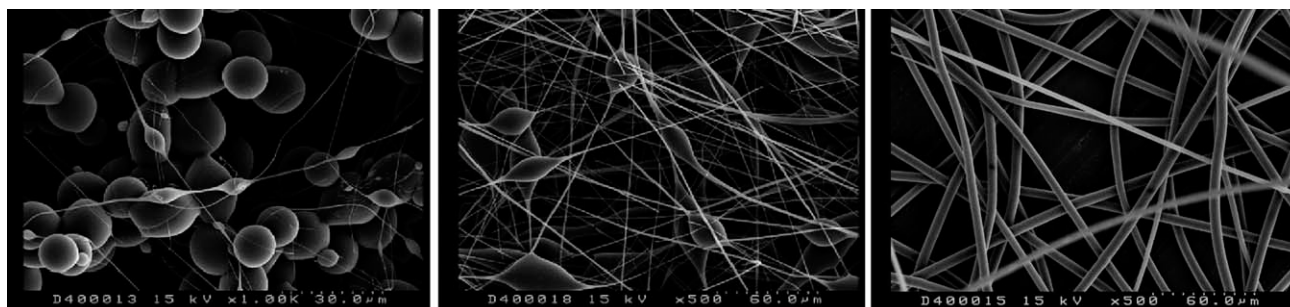
Figure 4 SEM images of the mats obtained from PDLA using a concentration of 10 wt % (left), 15 wt % (center), and 20 wt % (right).
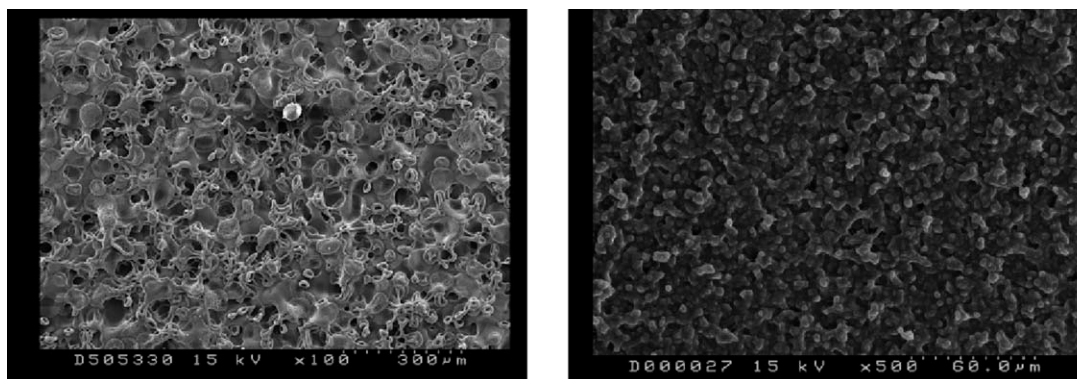
Figure 5 SEM images of the mats obtained from PLLA at 1 wt % (left) and PHV5 at 0.4 wt % (right).

solution had to be low. In an attempt to increase the CA of the surfaces, different mats were prepared using polymer concentrations lower than those described in Table II.

Two mats were obtained from PLLA and PHV5 using concentrations of 1 and 0.4 wt % that gave rise to water CAs of 98° and 126°, respectively. These angles were higher than those obtained in the flat surfaces obtained from the same polymers (PLLA 70° and PHV5 87°) but were clearly lower than those previously obtained using slightly higher concentrations.

The morphology of the mats obtained at low concentrations is displayed in Figure 5. As can be observed, the mats showed similar morphologies to those of a rough film, without beads or fibers. The reason for this observation was considered to be due to the nonevaporated solvent that at high solvent concentrations reached the collector destroying the generated roughness. This morphology was responsible for obtaining lower CAs. As a conclusion, it could be stated that below a limit concentration it was not possible to obtain hydrophobic surfaces because of the high solvent concentration.

CONCLUSIONS

The results of this work showed that the electrospinning technique allows the production of hydrophobic surfaces even in cases where hydrophilic polymers are used. The main factors that control the hydrophobic character are the polymer concentration and the crystallinity of the materials. Higher water

CAs were obtained using crystalline polymers. In addition, lower concentrations led to a bead-like morphology that increased the CA. However, below a limit concentration it was not possible to obtain hydrophobic surfaces because of the high solvent concentration.

References

1. Li, X. M.; Reinhoudt, D.; Crego-Calama, M. Chem Soc Rev 2007, 36, 1350.
2. Ma, M.; Hill, R. M. Curr Opin Colloid Interface Sci 2006, 11, 193.
3. Parkin, I. P.; Palgrave, R. G. J Mater Chem 2005, 15, 1689.
4. Cheng, I. T.; Rodac, D. E. Appl Phys Lett 2005, 86, 144101.
5. Qian, B. T.; Shen, Z. Q. Langmuir 2005, 21, 9007.
6. Furstner, R.; Barthlott, W.; Neinhuis, C.; Walzel, P. Langmuir 2005, 21, 956.
7. Venkateswara Rao, A.; Latthe, S. S.; Nadargi, N. Y.; Hirashima, H.; Ganesen, V. J Colloid Interface Sci 2009, 332, 484.
8. Chang, K. C.; Chen, Y. K.; Chen, H. J Appl Polym Sci 2008, 107, 1530.
9. Xie, Z.; Buschle-Diller, G. J Appl Polym Sci 2010, 115, 1.
10. Reneker, D. H.; Yarin, A. L. Polymer 2008, 49, 2387.
11. Buruaga, L.; Muñoz, M. E.; Irusta, L.; González, A.; Iruin, J. J. J Appl Polym Sci 2009, 114, 2922.
12. Zhu, M.; Zuo, W.; Yu, H.; Yang, W.; Chen Y. J Mater Sci 2006, 41, 3793.
13. Menini, R.; Farzaneh, M. Polym Int 2008, 55, 77.
14. Minglin, M.; Gupta, M.; Li, Z.; Zhai, K.; Gleason, K. K.; Cohen, R. E.; Rubner, M. F.; Rutledge, G. C. Adv Mater 2007, 19, 255.
15. Quiu, Z.; Yang, W.; Ikehara, T.; Nishi, T. Polymer 2005, 46, 11814.
16. Nakane, K.; Tamaki, C.; Hata, Y.; Ogihara, T.; Ogata, N. J Appl Polym Sci 2008, 108, 2139.
17. Buruaga, L.; Sardon, H.; Irusta, L.; González, A.; Fernández-Berridi, M. J.; Iruin, J. J. J Appl Polym Sci 2010, 115, 1176.
18. Xie, J.; Li, X.; Xia, Y. Macromol Rapid Commun 2008, 29, 1775.